Original Article

Theoretical deposition of variably sized platelets in the respiratory tract of healthy adults

Robert Sturm

Department of Material Sciences and Physics, Division of Physics and Biophysics, University of Salzburg, Salzburg, Austria
Correspondence to: Robert Sturm. Department of Material Sciences and Physics, Division of Physics and Biophysics, University of Salzburg, Hellbrunnerstrasse 34, A-5020 Salzburg, Austria. Email: sturm_rob@hotmail.com.

Background: Numerous types of airborne particles representing by-products of mechanical processes such as milling, abrading or polishing are characterized by platelet-like shapes. Besides these particles of the micrometer scale also nanoplatelets consisting of single or multiple layers of graphene sheets can be theoretically dispersed in the atmosphere. The present study describes the theoretical behavior of variably sized platelets in the airways of the human respiratory tract.

Methods: Aerodynamic characteristics of inhaled platelets belonging to the nano- or micrometer scale were approximated by application of the projected-area diameter concept describing particle orientation in the air-conducting lung structures and by calculation of the related aerodynamic diameter. Particle transport was assumed to take place in a stochastic lung architecture with respective variability of morphometric determinants in single airway generations. Deposition mechanisms used for the computations included Brownian motion, inertial impaction, interception, and gravitational settling. Calculations were conducted for three different breathing scenarios (sitting, light-exercise, and heavy-exercise breathing) and for platelets ranging in thickness from 10 nm to 1 µm and in maximal projected-area diameter from 1 to 30 µm.

Results: Under sitting breathing conditions platelets with a thickness of 10 nm deposit in the airways by 21% to 40%, whereby a "hot spot" of deposition can be observed in airway generation 20. In the case of platelets with a thickness of 100 nm, deposition fractions ranging from 20.9% to 78.3% (maximum in airway generation 20) can be predicted. Platelets adopting a thickness of 1 µm deposit in the airways by 54.2% to 99.6% (maximum in airway generation 21). Increase of the breathing intensity can have either a reducing or enhancing effect on local deposition.

Conclusions: Due to the partly high deposition fractions of platelets measured in the lung airways, these particles may bear the potential to act as serious health hazards that have to be subjected to further studies in the future.

Keywords: Dust particles; graphene nanoplatelets (GNP); inhalation; lung deposition; model; human respiratory tract

Received: 08 March 2018; Accepted: 30 March 2018; Published: 06 May 2018.
doi: 10.21037/amj.2018.04.03
View this article at: http://dx.doi.org/10.21037/amj.2018.04.03

Introduction

The ambient atmosphere normally includes numerous airborne particles belonging to different size and shape categories (1-3). Besides spherical particles representing only a small fraction of the total particulate mass transported in the air, also non-spherical particles as well as various aggregates and agglomerates may occur as respective aerosols. With regard to non-spherical particles, platelet-like geometries may be distinguished from fiber-like and completely irregular shapes (4,5). Within the class of platelets all kinds of dusts originating from numerous mechanical processes (e.g., crushing, milling, abrading, polishing) have to be evaluated as most prominent. Dust particles may be composed of a multitude of materials, whereby mineral dust primarily produced in mining

companies significantly differs from those dusts representing by-products of wood processing, cotton milling or meal production (6,7). Whilst most dust particles, which result from the processes noted above, are characterized by sizes falling within the micrometer scale, so-called graphene nanoplatelets (GNP) have a thickness of only 10 to 100 nm and thus may be attributed to the category of nano-scale particles (8-10). These particulate bodies, however, stand in the focus of modern nano-technology. Although they are produced under strict safety measures, they may be accidentally released into the atmosphere, where they may come into contact with the population (11).

From a medical point of view, inhalation of dust particles retrospects on a long scientific tradition (12), whereas investigations on the intrapulmonary behavior of GNP are still standing at the very beginning (8-10). Extensive inhalation of dusts, representing a negative side-effect at many industrial work places, may result in the development of respiratory diseases such as chronic bronchitis, bronchiectasis, silicosis or pneumoconiosis. In most of these cases metabolism in the lung tissues as well as processes related to gas exchange are irreversibly affected, which commonly leads to a significant decline of live quality (13-15). Inhalation of GNP is generally associated with several specificities. According to previous studies (8-10) these particles may penetrate in high numbers to the lung periphery, where they are preferentially deposited in the alveoli. Due to their extreme biopersistence and largely anisometric geometry, they mostly escape from macrophage clearance and enter the alveolar interstitial (16), where they may induce a multitude of intra- and extracellular reactions. Although a direct relationship between GNP deposition and lung cancer is devoid of any scientific basis hitherto, some references indicate a noxious potential of these particles, which is similar to that of asbestos fibers, man-made vitreous fibers (MMVF), and carbon nanotubes (CNT) (17-20).

Epidemiological and experimental studies describing the health effects of dust inhalation exist in sufficient number (6,7,12), whilst our knowledge on the behaviour of GNP is restricted to a few experiments with laboratory animals (8,9). Experimental work starting in the 1970s and 1980s was always accompanied by theoretical research setting its focus on the development of particle transport and deposition models (1-5,17-20). Meanwhile, mathematical approaches and related computer programs have attained a developmental stage, where respective predictions are marked by both high accuracy and increased reliability. Computer codes working with numerical and stochastic concepts are able to consider a multiplicity of frame conditions, among which non-spherical particle geometry is due to high significance (21-25).

In the present contribution intrapulmonary transport and deposition of variably sized platelets is examined in greater detail. For this purpose, particles ranging in thickness from 10 nm to 1 µm and in diameter from 1 to 30 µm were modeled with regard to their behaviour in the airways (extrathoracic air passages, airway generations 1 to 25) of the respiratory tract. The study among other pursues the goal to find a relationship between hitting probabilities on the one side and particle properties on the other, so that appropriate risk assessments with regard to the inhalation of platelets can be carried out on future.

Methods

Modeling aerodynamic properties of platelet-like particles

Theoretical description of the aerodynamic characteristics of inhaled platelets with different sizes was conducted according to the procedure outlined by Sturm (10) as well as Schinwald and co-authors (9). As proposed in these publications, irregularly shaped particles can be among other approximated by the so-called projected-area diameter. This hypothetical measure simply represents the diameter of a circle with identical area as the image of the particle projected on a horizontal plane. Mathematically, the projected-area diameter (d_{proj}) can be expressed by the equation

$$d_{proj} = 2 \cdot \sqrt{\left(\frac{d^2_{proj,\max}}{4} \cdot \pi \cdot \cos\varphi + d_{proj,\max} \cdot t \cdot \sin\varphi \right) / \pi} \quad [1],$$

Where $d_{proj,max}$ denotes the maximal projected-area diameter for the case of parallel orientation between platelet and projection plane, whilst φ represents the angle between platelet and projection plane and t the thickness of the particle. Based upon the above formula, a minimal projected-area diameter is certainly obtained in the case of φ adopting a value of 90°. For the simulations outlined in this contribution a uniform orientation of the inhaled platelets parallel to the stream lines was assumed, so that the maximal projected-area diameter was applied to the further computations. As already stated in numerous previous studies (1-7), the aerodynamic diameter (d_{ae}) has to be understood as a key measure of theoretical particle

aerodynamics, because it describes the diameter of a unit-density sphere with exactly the same aerodynamic properties as the particle of interest. From a mathematical point of view, it can be expressed by the equation

$$d_{ae} = \sqrt{\frac{9\pi}{16} \cdot \frac{\rho_p}{\rho_o} \cdot d_{proj} \cdot t} \quad [2],$$

with ρ_p and ρ_0, respectively, denoting the density of the particle and unit-density (1 g/cm^3). In this contribution particle density was supposed to adopt a uniform value of 1 g/cm^3, so that the density term in the equation noted above can be fully neglected.

For the theoretical computation of this study platelets with ideal cylindrical geometry were used. Thereby, thickness of the particles was varied between 0.01 and 1 µm, whereas the cylindrical diameter ranged from 1 to 30 µm. According to Eq. [2] aerodynamic diameters of thin platelets (0.01 µm) adopt values between 0.13 and 0.73 µm. The aerodynamic diameter of 0.1 µm thick platelets exhibits a variation between 0.42 and 2.30 µm. Finally, platelets with a thickness of 1 µm are characterized by aerodynamic diameters ranging from 1.33 to 7.28 µm. Whilst thin platelets have to be partly attributed to the transition flow regime, thicker particles completely belong to the continuum flow regime (1-5,26). In the latter case calculation of Cunningham slip correction factors was waived.

Deposition of variably sized platelets in the human respiratory tract

Simulation of platelet deposition in various regions of the human lungs was carried out by assuming (I) a stochastic architecture of the respiratory tract, (II) a generation of random particle transport paths through the bronchial airway structure, and (III) particle collision with bronchial and alveolar walls according to well-defined empirical, analytical, and numerical equations (27-30). Each platelet entering the respiratory system is immediately seized by four main deposition mechanisms (Brownian motion, sedimentation, inertial impaction, interception), whose intensity depends upon several physical properties of the particle (size, density) and the velocity of the inhaled aerosol in the tubular structures (27-30). For an appropriate statistical evaluation of the simulation results 10,000 particle paths and associated deposition scenarios were modelled for each platelet type used in this study. A significant increase of modeling efficiency was achieved by application of the Monte Carlo method and the mathematical technique of statistical weights (27). Besides total deposition denoting the overall fraction of inhaled particles captured in diverse structures of the respiratory tract, also regional (i.e., extrathoracic, bronchial, alveolar) and airway-generation-specific deposition were simulated.

Results

Total and regional deposition of platelets with variable size

Under sitting breathing conditions both total and regional depositions of platelets depend (I) on particle thickness and (II) on the maximal projected-area diameter. According to *Figure 1A*, platelets with a thickness of 0.01 µm deposit in the respiratory tract by 20.9% to 40.0%, with highest deposition probabilities being recognizable for smallest particles. A completely different picture can be drawn for platelets with thicknesses of 0.1 and 1.0 µm, where deposition probability is subject to a continuous increase with growing particle size. Concretely speaking, platelets with a thickness of 0.1 µm are accumulated in the respiratory tract by 20.9% to 78.3%, whereas platelets with a thickness of 1.0 µm show a deposition probability ranging from 54.2% to 99.6%.

With regard to extrathoracic deposition of variably sized platelets respective modelling results are summarized in *Figure 1B*. In general, any size-dependent trends worked out for total deposition can be again observed for particle accumulation in the extrathoracic (nasal) airways. Thereby, platelets with a thickness of 0.01 µm are deposited by 4.89% to 8.88%, whilst platelets with a thickness of 0.1 µm hit the airway walls by 5.02% to 45.80%. Platelets with a thickness of 1.0 µm, finally, deposit with a probability ranging from 21.9% to 94.8%. Deposition of variably sized platelets in the bronchial structures follows some different trends (*Figure 1C*). In the case of thinnest platelets (0.01 µm) deposition varies between 10.7% and 20.2%, whereby smaller particles again have the ability to produce higher percentages of bronchial hitting events. Platelets with a thickness of 0.1 µm deposit in the bronchial airways by 10.9% to 19.7% (positive correlation between size and deposition probability), and platelets with a thickness of 1.0 µm exhibit an accumulation between 4.05% and 19.7% (maximum for $d_{proj,max}$ =3 µm). Alveolar deposition depicted in *Figure 1D* also shows a dependence on platelet thickness and size, whereby thinnest platelets are deposited in the air

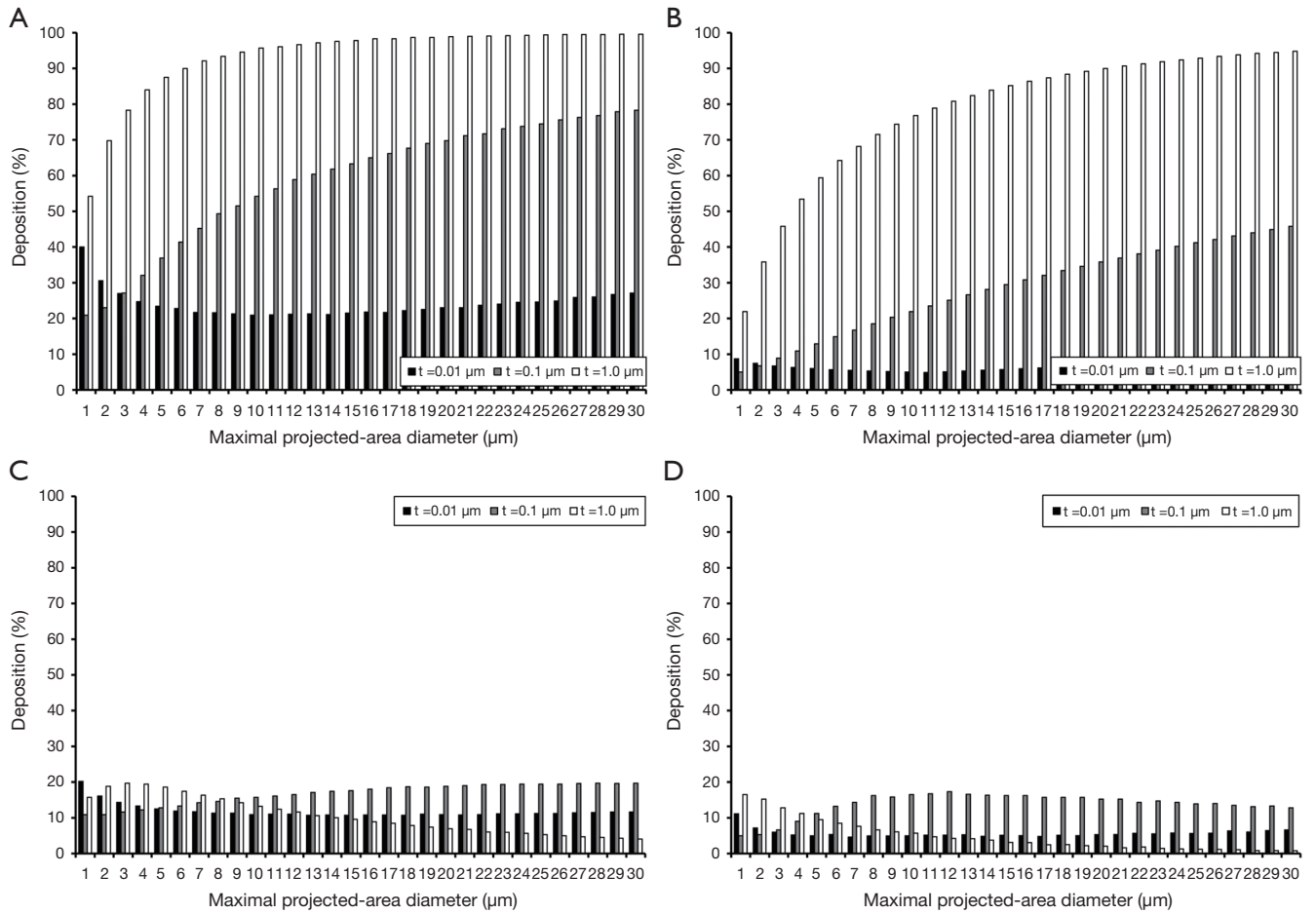

Figure 1 Theoretical deposition of cylindrical platelets with different thicknesses and maximal projected-area diameters under sitting breathing conditions. (A) Total deposition; (B) extrathoracic deposition; (C) bronchial deposition; (D) alveolar deposition.

sacs by 4.9% to 11.1%. Platelets with a thickness of 0.1 μm are distinguished by a deposition ranging from 4.98% to 17.1%, whereas platelets with a thickness of 1.0 μm hit the alveolar walls by 0.77% to 16.5%.

Airway generation-specific deposition of platelets with variable size

Deposition computations conducted for platelets with a thickness of 0.01 μm and maximal projected-area diameters of 1, 15, and 30 μm are summarized in *Figure 2A*. As can be clearly recognized from the graph, all particles are characterized by deposition probabilities of less than 1% in airway generations 0 to 12 and 24 to 30. In the remaining generations 13 to 23, deposition commonly produces a maximum, whose intensity depends on geometric particle properties. Platelets with $d_{proj,max}$ =1 μm have their maximal deposition in generation 20 (3.86%), whereas platelets with $d_{proj,max}$ =15 μm indeed produce their deposition maximum at the same lung site but accumulate there with only 2.01%. Platelets with $d_{proj,max}$ =30 μm deposit in airway generation 20 by 2.18%.

Platelets with a thickness of 0.1 μm and the same maximal projected-area diameters used above show rather similar deposition behaviour with respect to their thinner counterparts. In this case deposition maxima can be localized in airway generations 20 and 21. Maximal deposition values amount from 2.01% ($d_{proj,max}$ =1 μm) over 4.21% ($d_{proj,max}$ =30 μm) to 4.54% ($d_{proj,max}$ =15 μm; *Figure 2B*). Concerning platelets with a thickness of 1.0 μm, deposition of particles with $d_{proj,max}$ =1 μm reaches a maximal value of 4.28% (generation 21). Particles with $d_{proj,max}$ =15 μm

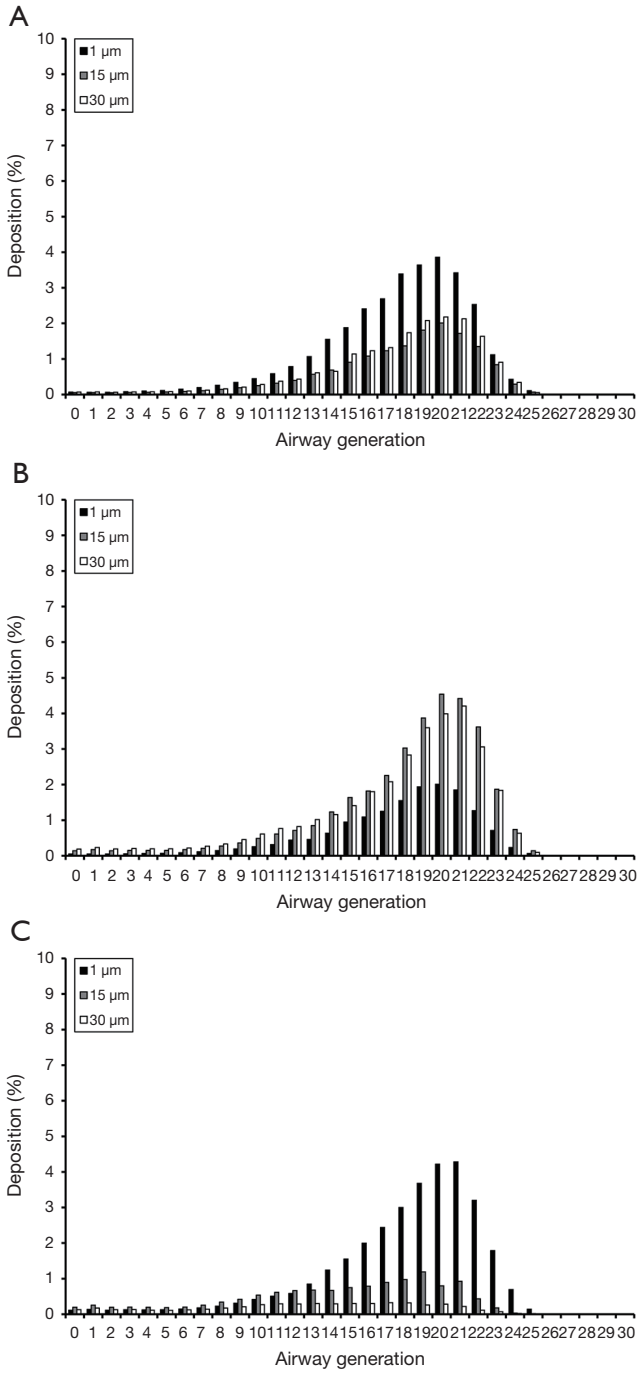

Figure 2 Airway-generation-specific deposition of platelets with maximal projected-area diameters of 1, 15, and 30 µm under sitting breathing conditions. (A) Thickness of 0.01 µm; (B) thickness of 0.1 µm; (C) thickness of 1.0 µm.

exhibit a maximal deposition of 1.19% (generation 19), whilst accumulation of particles with $d_{proj,max}$ =30 µm continuously adopts values of less than 1% (*Figure 2C*).

Dependence of platelet deposition on inhalation flow rate

In general, deposition of particles in the human respiratory tract is controlled to a high extent by the intensity of breathing. Therefore, light-work and heavy-work breathing conditions produce other particle deposition patterns than sitting breathing scenarios. For platelets with different thicknesses and maximal projected-area diameters this phenomenon is summarized in *Figures 3-6*. Basically, any intensification of inhalation, which is expressed by higher tidal volumes and flow rates of the inspired air, is characterized by a decrease of total deposition for platelets adopting a thickness of 0.01 µm and by an increase of total deposition for the other two thickness categories used in this study. Similar observations as for total deposition can be commonly made for extrathoracic deposition. In the case of bronchial and alveolar accumulation of platelets with thicknesses of 0.1 and 1.0 µm, respective trends documented for sitting breathing conditions are significantly intensified during light-work breathing, but become again attenuated during heavy-work breathing. Bronchial and alveolar deposition of platelets with a thickness of 0.01 µm, on the other hand, is subject to a continuous reduction with any intensification of the inhalation flow rate (*Figures 3,4*).

The dependence of regional particle deposition on breathing conditions is also reflected in the airway-generation-specific deposition patterns exhibited in *Figures 5,6*. Concretely speaking, platelets with a thickness of 0.01 µm undergo a continuous reduction of deposition with increasing inhalation flow rate. This diminution has very similar extents for small ($d_{proj,max}$ =1 µm) and large particle ($d_{proj,max}$ =30 µm). Platelets with thicknesses of 0.1 and 1.0 µm, respectively, are marked by enhanced accumulation in the airways after transition from sitting to light-work breathing, whereas transition from light-work to heavy-work breathing is again associated with a decrease in deposition of the inhaled particles.

Discussion

As demonstrated in numerous scientific publications (1-10,31-37), airborne particles adopting platelet-like geometry

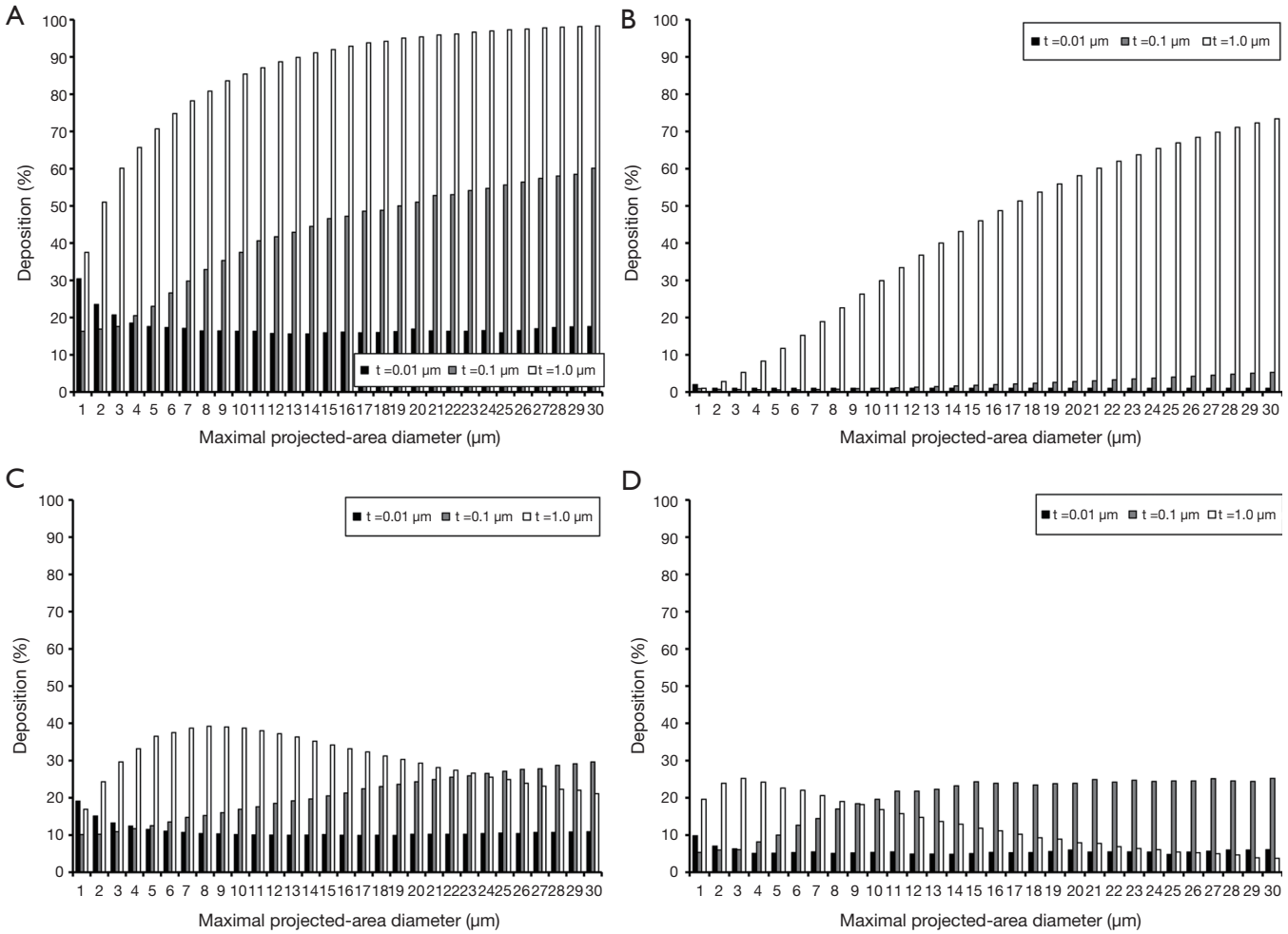

Figure 3 Theoretical deposition of cylindrical platelets with different thicknesses and maximal projected-area diameters under light-work breathing conditions. (A) Total deposition; (B) extrathoracic deposition; (C) bronchial deposition; (D) alveolar deposition.

may occur with high concentrations in the environmental atmosphere. This circumstance mainly concerns particles of the micrometer scale, because many mechanical processes of the industrial-scale produce irregularly shaped dusts of this size category that are spread into the air in high amounts. With regard to platelets of the nano-scale the situation is represented differently insofar as respective particles such as graphene GNP are generated in hermetically sealed areas, from where they can be only released into the atmosphere by accident (8-10). Although GNP do not play an essential role in occupational medicine yet, possible health effects of these particles after their theoretical inhalation are nevertheless of invaluable asset (8-10).

The hypothetical simulations presented in this contribution could clearly demonstrate that platelet-shaped particles may occupy all regions of the respiratory tract. The amount of platelets being accumulated in a certain lung structure such as the extrathoracic airways, bronchi and bronchioles or alveoli depends upon a multiplicity of physical and physiological factors. Among the physical determinants particle size, represented by the aerodynamic diameter, has the most significant effect on total, regional and local deposition of the platelets. As found by a multitude of studies published in the distant and recent past (12,17-20), relationship between total particle deposition and particle size is commonly expressed by a U-shaped curve with high deposition values occurring for very small (<10 nm) and large particles (>5 μm), but low deposition being observable for particulate substances of intermediate size (0.1–1 μm). Platelets and ideal spheres with identical circular diameter

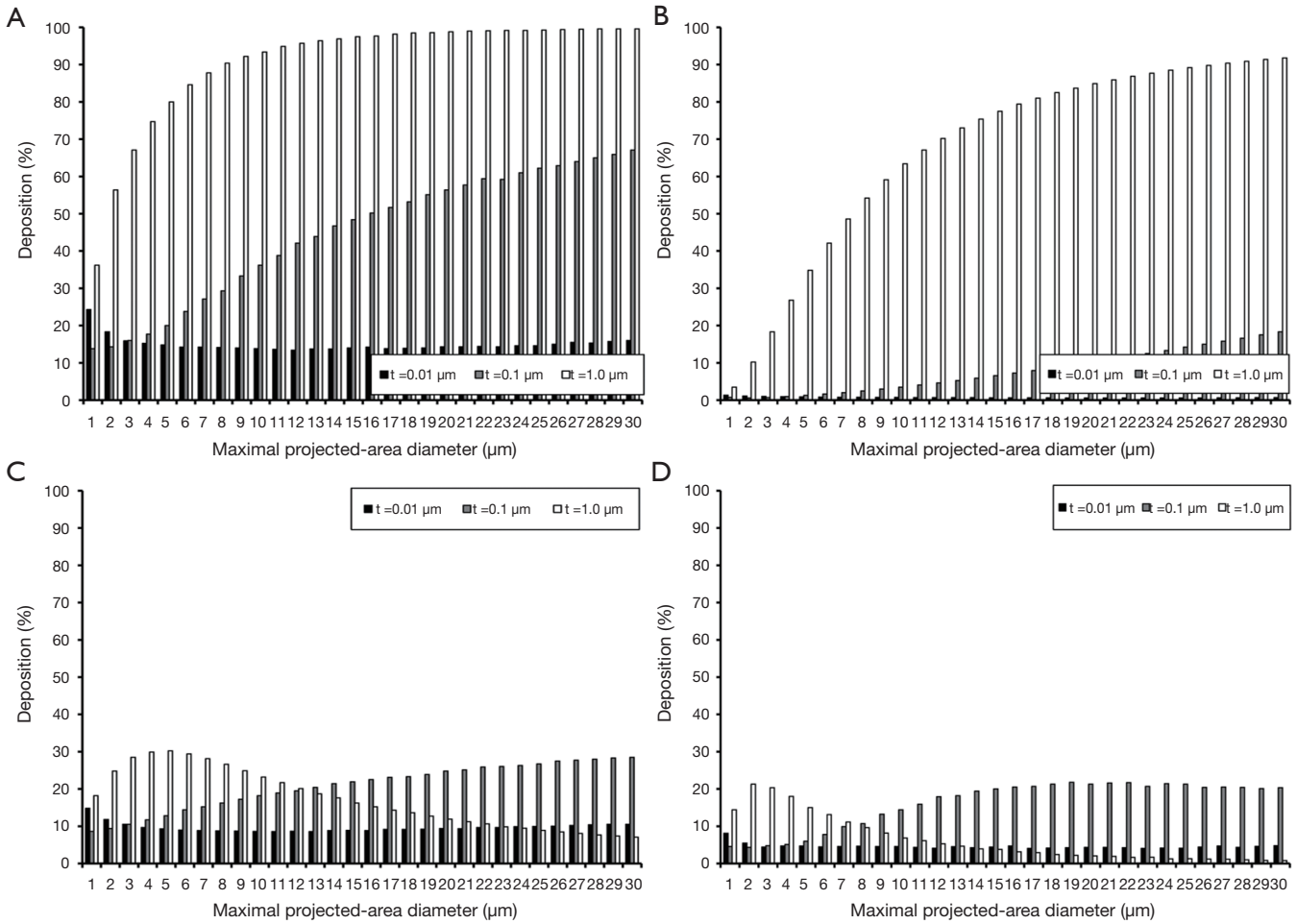

Figure 4 Theoretical deposition of cylindrical platelets with different thicknesses and maximal projected-area diameters under heavy-work breathing conditions. (A) Total deposition; (B) extrathoracic deposition; (C) bronchial deposition; (D) alveolar deposition.

(e.g., 10 μm) partly exhibit immense differences with regard to their aerodynamically relevant size: Whilst the spherical particle shows an aerodynamic diameter of 10 μm, a platelet with a thickness of 10 nm disposes of an aerodynamic diameter of only 0.42 μm and thus represents a preferred target for forces taking place on the molecular level (1-4,26). A complete picture, however, is drawn for platelets with a thickness of 1 μm, which adopt an aerodynamic diameter of 4.2 μm and are therefore preferentially seized by mass-related forces (10-12). In general, thin platelets with small diameters are mainly deposited in the upper parts of the respiratory tract. Any increase of the lateral particle dimensions results in a dislocation of deposition towards the lung periphery (10). For platelets with intermediate (0.1 μm) and enhanced thickness (1 μm) reverse deposition effects may be recognized: whilst particles with small diameters are characterized by high deposition intensities in central and distal lung structures, platelets with large diameters again tend to be accumulated in the upper airways of the respiratory tract. Concerning their deposition behaviour thin platelets share some commonalities with CNT, where single-walled representatives are preferably deposited in the upper lung, multi-walled representatives, on the other hand, more likely penetrate to the deeper lung (17-21).

The influence of breathing physiology on platelet deposition in the respiratory tract is best portrayed in terms of the tidal volume and the time used for inhalation of this air capacity (18-21). Previous investigations carried out on variably sized and shaped particles (2-4,36,37) could already demonstrate that any increase of the inhalation

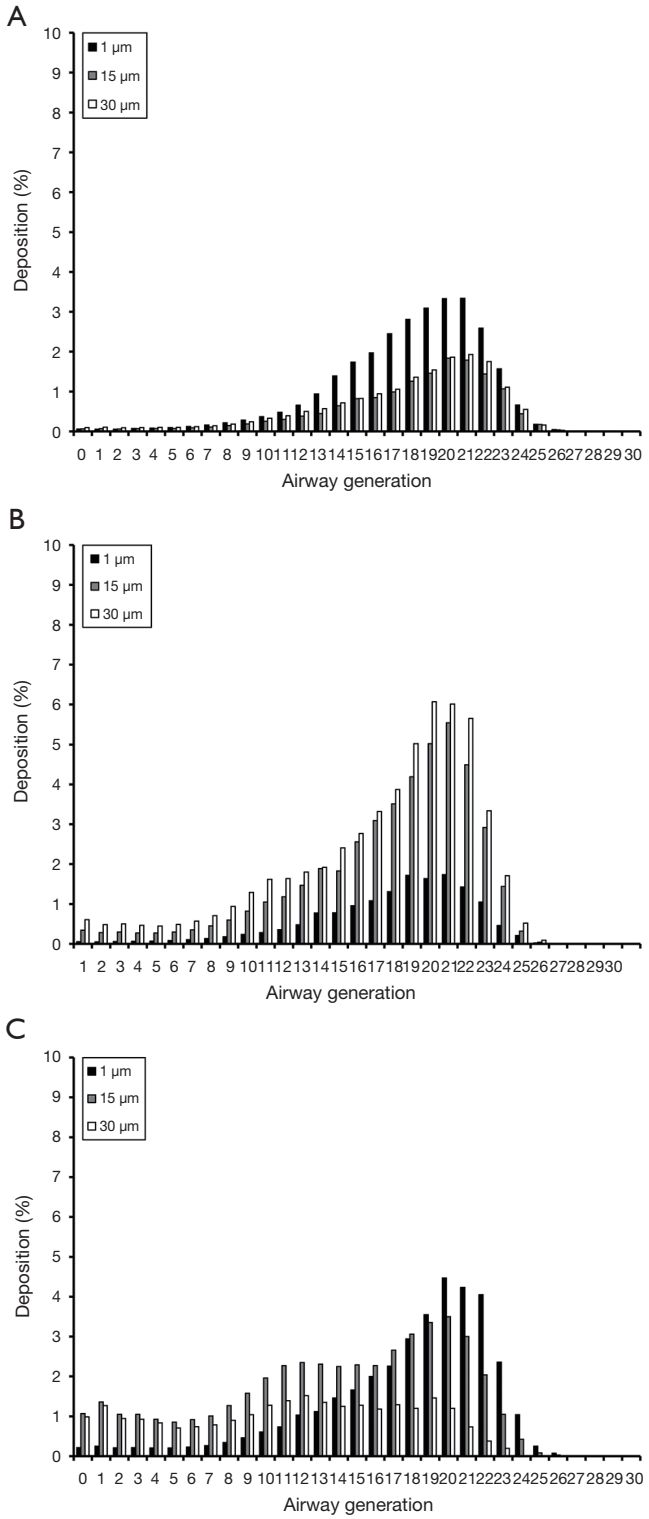

Figure 5 Airway-generation-specific deposition of platelets with maximal projected-area diameters of 1, 15, and 30 μm under light-work breathing conditions. (A) Thickness of 0.01 μm; (B) thickness of 0.1 μm; (C) thickness of 1.0 μm.

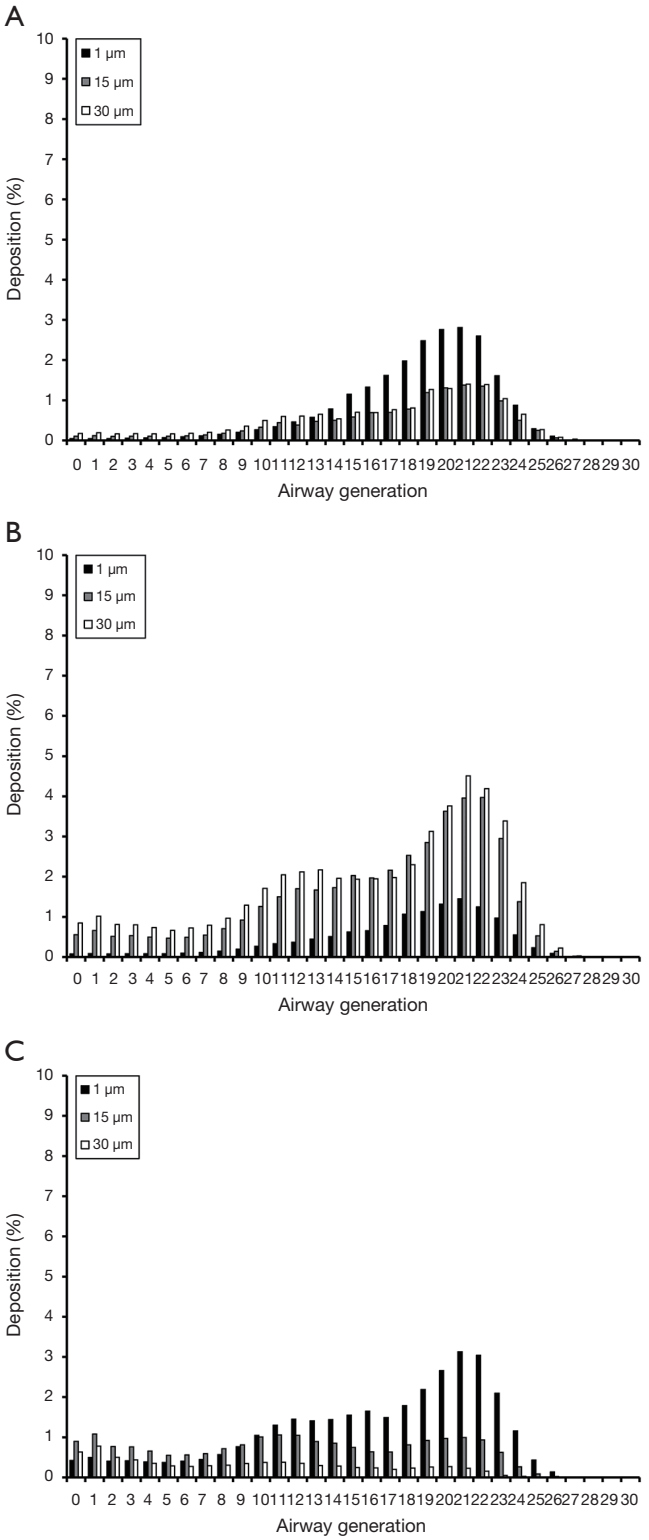

Figure 6 Airway-generation-specific deposition of platelets with maximal projected-area diameters of 1, 15, and 30 μm under heavy-work breathing conditions. (A) Thickness of 0.01 μm; (B) thickness of 0.1 μm; (C) thickness of 1.0 μm.

flow rate causes a dislocation of small particle deposition towards more peripheral structures of the lung. In the case of intermediately sized and large particles a reverse effect with enhanced deposition in the upper airway structures was described. In the case of platelets belonging to three thickness categories, breathing intensity has different influences on particle deposition. Very thin platelets (0.01 µm) commonly undergo a reduced deposition, whereas platelets with intermediate to enhanced thickness are characterized by a reverse effect. This phenomenon equally concerns total, regional, and airway-generation-specific deposition. The theoretical results are largely confirmed by experiments, which have used small to intermediately sized particles and different breathing conditions (12). In general, particles belonging to the nanometer scale are mainly affected by Brownian motion, whose effectiveness declines with the velocity of the inhaled air stream (12). Larger particulate bodies, on the other side, are chiefly influenced by mass-related deposition mechanisms, whose efficiency positively correlates with the volume and flow rate of the inspired air (27-30).

Conclusions

From the results presented in this contribution it may be concluded that platelets bear the potential of serious accumulation at different lung sites, whereby alveolar deposition, being of high interest in medical respects, can adopt rather high percentages. The number of particles hitting the alveolar walls, however, depends on both physical and physiological factors and thus has to be subjected to further detailed analyses in near future.

Acknowledgements

Funding: None.

Footnote

Conflicts of Interest: The author has completed the ICMJE uniform disclosure form (available at http://dx.doi.org/10.21037/amj.2018.04.03). The author has no conflicts of interest to declare.

Ethical Statement: The author is accountable for all aspects of the work in ensuring that questions related to the accuracy or integrity of any part of the work are appropriately investigated and resolved.

References

1. Kasper G. Dynamics and measurement of smokes. I Size characterization of nonspherical particles. Aerosol Sci Technol 1982;1:187-99.
2. Sturm R. Modellrechnungen zur Deposition nicht-sphärischer Teilchen in den oberen Luftwegen der menschlichen Lunge. Z MedPhys 2009;19:38-46.
3. Sturm R. Theoretical models of carcinogenic particle deposition and clearance in children's lungs. J Thorac Dis 2012;4:368-76.
4. Sturm R. Theoretical models for dynamic shape factors and lung deposition of small particle aggregates originating from combustion processes. Z Med Phys 2010;20:226-234.
5. Sturm R. Inhaled nanoparticles. Phys Today 2016;69:70-1.
6. Sturm R. Theoretical and experimental approaches to the deposition and clearance of ultrafine carcinogens in the human respiratory tract. Thoracic Cancer 2011;2:61-8.
7. Sturm R. Theoretical models of carcinogenic particle deposition and clearance in children's lungs. J Thorac Dis 2012;4:368-76.
8. Sanchez VC, Jachak A, Hurt RH, et al. Biological interactions of graphene-family nanomaterials – an interdisciplinary review. Chem Res Toxicol 2012;25:15-34.
9. Schinwald A, Murphy FA, Jones A, et al. Graphene-based nanoplatelets: a new risk to the respiratory system as a consequence of their unusual aerodynamic properties. ACS Nano 2012;6:736-46.
10. Sturm R. Inhalation of nanoplatelets – Theoretical deposition simulations. Z Med Phys 2017;27:274-84.
11. Novoselov KS, Geim AK, Morozov SV, et al. Electric field effect in atomically thin carbon films. Science 2004;306:666-9.
12. International Commission on Radiological Protection (ICRP). Human respiratory tract model for radiological protection, Publication 66. Oxford: Pergamon Press, 1994.
13. Donaldson K, Aitken R, Tran L, et al. Carbon nanotubes: a review of their properties in relation to pulmonary

toxicology and workplace safety. Toxicol Sci 2006;92:5-22.
14. Poland CA, Duffin R, Kinloch I, et al. Carbon nanotubes introduced into the abdominal cavity of mice show asbestos-like pathogenicity in a pilot study. Nat Nanotechnol 2008;3:423-8.
15. Duffin R, Clouter A, Brown D, et al. The importance of surface area and specific reactivity in the acute pulmonary inflammatory response to particles. Ann Occup Hyg 2002;46:242-5.
16. Sturm R. A computer model for the simulation of fiber-cell interaction in the alveolar region of the respiratory tract. Comput Biol Med 2011;41:565-73.
17. Sturm R, Hofmann W. A theoretical approach to the deposition and clearance of fibers with variable size in the human respiratory tract. J Hazard Mater 2009;170:210-8.
18. Sturm R. Nanotubes in the human respiratory tract—Deposition modelling. Z Med Phys 2015;25:135-45.
19. Sturm R. Spatial visualization of theoretical nanoparticle deposition in the human respiratory tract. Ann Transl Med 2015;3:326.
20. Sturm R. A stochastic model of carbon nanotube deposition in the airways and alveoli of the human respiratory tract. Inhal Toxicol 2016;28:49-60.
21. Högberg SM. Modeling nanofiber transport and deposition in human airways. Lulea, Sweden: Tech Univ Lulea, 2010.
22. Sturm R, Hofmann W. A computer program for the simulation of fiber deposition in the human respiratory tract. Comput Biol Med 2006;36:1252-67.
23. Sturm R. Deposition and cellular interaction of cancer-inducing particles in the human respiratory tract: Theoretical approaches and experimental data. Thoracic Cancer 2010;1:141-52.
24. Sturm R. A computer model for the simulation of fiber-cell interaction in the alveolar region of the respiratory tract. Comput Biol Med 2011;41:565-73.
25. Sturm R. Theoretical approach to the hit probability of lung-cancer-sensitive epithelial cells by mineral fibers with various aspect ratios. Thoracic Cancer 2010;1:116-25.
26. Willeke K, Baron PA. Aerosol measurement. New York: John Wiley, 1993.
27. Koblinger L, Hofmann W. Monte Carlo modeling of aerosol deposition in human lungs. Part I: Simulation of particle transport in a stochastic lung structure. J Aerosol Sci 1990;21:661-74.
28. Ingham DB. Diffusion of aerosol from a stream flowing through a cylindrical tube. J Aerosol Sci1975;6:125-32.
29. Yeh HC, Schum GM. Models of the human lung airways and their application to inhaled particle deposition. Bull Math Biol 1980;42:461-80.
30. Zhang L, Asgharian B, Anjilvel S. Inertial and interceptional deposition of fibers in a bifurcating airway. J Aerosol Med 1996;9:419-30.
31. Hofmann W, Sturm R, Winkler-Heil R et al. Stochastic model of ultrafine particle deposition and clearance in the human respiratory tract. Radiat Prot Dosimetry 2003;105:77-80.
32. Sturm R. A computer model for the simulation of nanoparticle deposition in the alveolar structures of the human lungs. Ann Transl Med 2015;3:281.
33. Sturm R. Modeling the deposition of bioaerosols with variable size and shape in the human respiratory tract - A review. J Adv Res 2012;3:295-304.
34. Sturm R. Bioaerosols in the lungs of subjects with different ages - part 1: deposition modeling. Ann Transl Med 2016;4:211.
35. Sturm R. Theoretical models for the simulation of particle deposition and tracheobronchial clearance in lungs of patients with chronic bronchitis. Ann Transl Med 2013;1:3.
36. Sturm R. Computer-aided generation and lung deposition modeling of nano-scale particle aggregates. Inhal Toxicol 2017;29:160-8.
37. Sturm R. Carbon nanotubes in the human respiratory tract–clearance modeling. Ann Work Expo Health 2017;61:226-36.

doi: 10.21037/amj.2018.04.03
Cite this article as: Sturm R. Theoretical deposition of variably sized platelets in the respiratory tract of healthy adults. AME Med J 2018;3:61.

